Speed of ion-trap quantum-information processors

A. Steane,[1] C. F. Roos,[2] D. Stevens,[1] A. Mundt,[2] D. Leibfried,[2] F. Schmidt-Kaler,[2] and R. Blatt[2]
[1]*Oxford Centre for Quantum Computation, Department of Physics, University of Oxford, Clarendon Laboratory, Parks Road, Oxford OX1 3PU, England*
[2]*Institut für Experimentalphysik, Universität Innsbruck, A-6020 Innsbruck, Austria*
(Received 17 March 2000; published 11 September 2000)

We investigate theoretically the speed limit of quantum gate operations for ion trap quantum information processors. The proposed methods use laser pulses for quantum gates that entangle the electronic and vibrational degrees of freedom of the trapped ions. Two of these methods are studied in detail and for both of them the speed is limited by a combination of the recoil frequency of the relevant electronic transition, and the vibrational frequency in the trap. We have experimentally studied the gate operations below and above this speed limit. In the latter case, the fidelity is reduced, in agreement with our theoretical findings.

PACS number(s): 03.67.Lx, 32.80.Lg, 32.80.Qk

I. INTRODUCTION

Experimental methods that allow both coherent control, and rapid and reliable measurement of the quantum state, have been available for some time for single ions held in ion traps. In an influential paper, Cirac and Zoller [1] showed furthermore how laser manipulation of a string of ions in a linear ion trap can achieve general coherent evolution of the joint state of the ions, using currently available technologies, and with good scaling properties. Specifically, the coherent evolution can be driven so as to realize any unitary transformation on the joint state of the ions, including transitions from product states to entangled states. Soon after their theoretical work, the essential ingredients of the method were realized experimentally for a single trapped ion [2], and more recently two ions were driven from a product state to an entangled state with around 90% fidelity using closely related ideas [3]. The entanglement is created without the need to use a random process, in contrast to other experimental approaches.

The combination of universal driven unitary evolution, an exponential scaling of the available Hilbert space with system size, and reliable measurement of the resulting state, are the essential ingredients for a future quantum computer. The scaling of system size in this argument is measured by the way the whole physical apparatus becomes larger, and operation of quantum logic gates slower, as more qubits are added to the system. In the case of the linear ion trap, the adding of further qubits (ions) into the trap is straightforward. The growth of the physical apparatus, and the slowing down of the processing, is dominated by the optical and electronic equipment needed to control the ions. This growth and slowdown is a polynomial, not exponential, function of the number of qubits, for small numbers of qubits. Technical problems will place a limit, as yet unknown, on the highest number of qubits that might be feasible, but below this limit the ion trap has the good scaling properties that allow the essential principles of quantum computing to be experimentally realized. Hence, laser-cooled ion-trap experiments have a dual interest both for studying new avenues in atomic physics (e.g., interferometry with entangled particles) and for understanding quantum information processing in a specific realizable system.

In this paper, we examine, both theoretically and experimentally, the speed with which general processing operations can be driven in the ion-trap system. We are concerned with the intrinsic limitations imposed by the physics of the system, such as the tightness of the trap and the presence of a rich energy-level structure in the vibrational modes. The initial proposal of Cirac and Zoller showed how to drive quantum operations in the limit of small Rabi frequency (slow operations), and initial experiments have been in this limit. Our aim here is to clarify the tradeoff between precision and speed of the quantum logic gates, and to derive the optimal way to operate the processor. This optimum is a compromise between speed-associated problems such as off-resonant excitation of unwanted transitions, and the basic decoherence rate due to environmental coupling that will limit the performance when the gates are too slow. Our main observation is to confirm the statement in [4], that the maximum gate rate obtained by the Cirac-Zoller method scales as the geometric mean of the trap vibrational frequency and the recoil frequency associated with the multi-ion string. This is in contrast to statements made elsewhere that the maximum gate rate is roughly proportional to the vibrational frequency, though this faster rate may be available if further tricks are adopted, such as excitation in the node of a laser standing wave [1]. We extend the discussion in [4] by making a quantitative statement, Eq. (20), of the relation between speed and precision of the gate.

We also calculate the maximum gate rate for the method proposed by Monroe *et al.* [5], where a controlled-not operation is achieved without the need for an additional transition and laser frequency, by driving multiple Rabi cycles on the carrier, for well-chosen values of the Lamb-Dicke parameter.

We experimentally study the Cirac-Zoller method, using a single trapped Calcium ion cooled to the ground state of the motion in one dimension. The experiments are akin to those in [2,6] where the methods were first demonstrated for one ion, except that we examine the regime as yet unexplored, where the gate rate is above the recoil frequency, so that the calculations carried out in the small Rabi frequency limit are no longer appropriate.

TABLE I. Matrix element for vibrational-state-changing transitions.

C_{nm}	0	1	2	3
0	1	$i\eta$	$-\eta^2/\sqrt{2}$	$-i\eta^3/\sqrt{6}$
1	$i\eta$	$(1-\eta^2)$	$i\sqrt{2}\eta(1-\eta^2/2)$	$-\sqrt{3/2}\eta^2(1-\eta^2/3)$
2	$-\eta^2/\sqrt{2}$	$i\sqrt{2}\eta(1-\eta^2/2)$	$(1-2\eta^2+\eta^4/2)$	$i\sqrt{3}\eta(1-\eta^2+\eta^4/6)$
3	$-i\eta^3/\sqrt{6}$	$-\sqrt{3/2}\eta^2(1-\eta^2/3)$	$i\sqrt{3}\eta(1-\eta^2+\eta^4/6)$	$1-3\eta^2+3\eta^4/2-\eta^6/6$

The paper is set out as follows. Section II presents the theory of the logic gates, and calculations of their fidelity as a function of the main parameters, primarily the Rabi frequency of the atom-light interaction, and the trap tightness. The calculations involve numerical solution of the Schrödinger equation for the system. We note the need to tune the laser light to the resonant frequency correctly, that is, taking into account the light shift (ac Stark shift) of the levels. We present results in the first instance considering only one mode of vibration of the ion string, and then in Sec. II G we briefly discuss the influence of the other modes. Section III presents our experiments. We cool a single trapped calcium ion to the ground state of the motion in one dimension, and then observe Rabi flopping on the first blue motional sideband of the narrow 729-nm transition. By driving the sideband in the regime where the Rabi frequency is of the order of the trap vibrational frequency, we observe the expected tradeoff between speed and precision of the operations, caused by off-resonant excitation of unwanted motional states.

II. THEORY OF SWITCHING RATE

A. Preliminaries

Consider a string of two or more ions in a linear trap. The trap is strongly confining along x and y directions, and less strongly confining along the z axis. We will assume motion in x and y directions is unexcited, and consider one normal mode of vibration of the ion string along z, writing its angular frequency ω_z. The other normal modes along z will be assumed to be unexcited throughout. (We will consider the element of approximation introduced by this assumption at the end.) For brevity, we will refer to this vibrational degree of freedom as ''the normal mode'' or ''the vibration.'' It has an evenly spaced ladder of energy levels $E_n=(n+1/2)\hbar\omega_z$. Typically, in an experiment one would choose the mode of interest to be the second or third, i.e., $\omega_z=\sqrt{3}\omega_{z,\mathrm{cm}}$ or $\sqrt{29/5}\omega_{z,\mathrm{cm}}$, where $\omega_{z,\mathrm{cm}}$ is the frequency of the center-of-mass mode. For modes other than the center of mass, the Lamb-Dicke parameter describing the ion-light coupling will vary from one ion to another [7], but this presents no problem as long as it is taken into account when choosing laser pulse intensities and/or durations. We will assume that the laser light is directed onto one ion at a time.

The Lamb-Dicke parameter is $\eta=\eta_1/\sqrt{N}$, where N is the number of ions, and $\eta_1=\sqrt{E_R/\hbar\omega_z}$. $E_R=(r\hbar k_z)^2/(2M)$ is the recoil energy for a single ion initially at rest undergoing a π pulse interaction with the laser field; k_z is the z component of the wave vector $\mathbf{k}$ of the laser field, M is the mass of the ion, and $r=1$ for a single-photon transition, and $r=2$ for a Raman transition assuming the geometry $k_{1z}=-k_{2z}$ for the two Raman beams. Examples of recoil frequencies E_R/h are given in Table II.

We will assume throughout that $\eta<1$. This is the regime in which the ion-trap processor is used in practice, both because it facilitates the initial cooling to the ground state of motion, and because the processor then runs faster, as we will discuss.

The Cirac-Zoller method adopts the internal state of each ion as a qubit (we restrict attention to two internal states and thus one qubit per ion). Gates between qubits are obtained via excitation of the common vibrational mode, and measurement of the state of one or more qubits is by observing fluorescence. The method uses the fact that arbitrary single-qubit rotations, combined with any one two-qubit gate such as controlled-not (^CX) or controlled-rotation (^CZ), between arbitrary pairs of qubits, form a universal set [8–10]. That is, any unitary transformation can be decomposed into elements from the set. In the trapped ion system, a single-qubit rotation is a transition in the internal state of a single ion, driven by a laser pulse. A ^CX between the internal states of any pair of ions A and B is achieved by a swap (S) operation between the internal state of A and the vibration, followed by ^CX between the vibration and the internal state of ion B (with vibration as control, ion internal state as target) followed by S again on ion A. Therefore, the only operations that will concern us are single-qubit rotations, and S and ^CX between a single ion and the vibration. All of these are achieved by excitation of a chosen transition. The unwanted off-resonant excitation of other transitions are the main subject of this paper.

The strength of the ion-laser interaction is parametrized by the Rabi frequency, given by

$$\Omega_{nm}=\langle n|\exp(i\eta(\hat{a}^\dagger+\hat{a}))|m\rangle\Omega_{\mathrm{free}} \tag{1}$$

$$\equiv C_{nm}\Omega, \tag{2}$$

where Ω_{free} is the Rabi frequency for a free ion, the states $|n\rangle$ are vibrational energy eigenstates, $\Omega=\exp(-\eta^2/2)\Omega_{\mathrm{free}}$, and the factor C_{nm} is given by the following Eq. (3). Values of C_{nm} are listed in Table I for the low-lying vibrational levels.

$$C_{nm}=\sqrt{m!n!}(i\eta)^{|f-m|}\times\sum_{j=0}^{\min(m,n)}\frac{(-1)^j\eta^{2j}}{j!(j+|n-m|)!(\min(m,n)-j)!}. \tag{3}$$

The single-qubit rotations can be much faster than the two-qubit gates, because the energy separation $\hbar\omega_0$ of the internal energy levels is much larger than that of the vibrational levels, and by choosing a laser-beam direction $k_z=0$ (single-photon transition) or $k_{1z}=k_{2z}$ (Raman transition), the Lamb-Dicke parameter can be made to vanish during single-qubit operations, which means these operations do not couple to the vibrational state (C_{nm} becomes δ_{nm}). Therefore, for $\Delta n=0$, Ω can be large compared to ω_z without causing off-resonant excitation of $\Delta n\neq 0$ transitions. Therefore, the speed of the ion-trap processor is limited by the S and ${}^{C}X$ gates.

The S gate is achieved by a π pulse on either the first red vibrational sideband, that is, at frequency $\omega_0-\omega_z$, or the first blue vibrational sideband at frequency $\omega_0+\omega_z$. The duration of the S gate is therefore

$$T_S=\frac{\pi}{\eta\Omega}, \tag{4}$$

where the gate becomes exact in the limit $\Omega\to 0$. The choice of red or blue sideband can be dictated by experimental convenience. The two are equivalent in terms of their quantum computational effect, since the logical operations produced can be made identical simply by relabeling the states (i.e., changing which internal state of the ion is called 0, and which is called 1). We will treat the red sideband throughout our theoretical discussion, but the results will apply equally to blue-sideband excitation. In fact, we used a blue sideband in the experiments described in Sec. III.

We will consider two methods for the ${}^{C}X$gate. The first is that described in the original proposal of Cirac and Zoller, where ${}^{C}X$ is obtained by single-bit rotations (Hadamard gates) combined with ${}^{C}Z$, and ${}^{C}Z$ is obtained from a 2π pulse on the first red sideband (or blue, depending on the relative positions of the levels) of an auxiliary transition in the ion, i.e., laser frequency $\omega_{\rm aux}-\omega_z$, gate duration

$$T_{C1}=\frac{2\pi}{\eta\Omega}. \tag{5}$$

The other method is that of Monroe *et al.* [5], who proposed using a $2m\pi$-pulse on the carrier (frequency ω_0), where m is an integer and $\eta^2=1/(2m)$. This is especially useful if an auxiliary transition is not available. When the vibrational state is $|n=0\rangle$, this drives an integer number of Rabi oscillations of the internal state, while if the vibrational state is $|n=1\rangle$, this drives a half-integer number of Rabi oscillations, since $C_{11}=1-\eta^2=(2m-1)/(2m)$. The method requires η to be fixed in the experiment to one of the special values $1/\sqrt{2m}$, which is easily done in practice by adjusting the trap confinement and/or laser-beam direction. The duration of a ${}^{C}X$ gate by the Monroe method is

$$T_{C2}=\frac{2m\pi}{\Omega}=\frac{\pi}{\eta^2\Omega}. \tag{6}$$

Since the ion trap is operated with $\eta<1$, it might be thought that T_{C2} is necessarily greater than T_{C1}. In fact, this is not necessarily the case, since these gate times are limited by the maximum allowable Rabi frequency Ω, and this can depend on the type of gate.

Sorensen and Molmer [11,12] have proposed a general method to implement gates such as controlled-not using bichromatic laser fields, achieving good fidelity even when the vibrational degrees of freedom are not in their ground state. The speed limitations of this method have recently been reexamined [13], so we will not discuss it here, other than to say the method appears to be useful.

B. Solution of time-dependent Schrödinger equation

Our aim is to find the maximum switching speed of the processor. It is seen from Eqs. (4)–(6) that this is determined by the maximum allowable Rabi frequency during the gates that operate on the vibrational state. The Rabi frequency cannot be arbitrarily large, because in the limit $\Omega\gg\omega_z$, the evolution would be independent of the vibrational state.

In order to find the maximum Rabi frequency, we need to solve the time-dependent Schrödinger equation for the system, without making the approximation of small Ω. We assume a two-level ion. This means we will not explicitly examine the type of ${}^{C}X$ gate that uses an auxiliary level [Eq. (5)], but in any case this operation is closely related to the S operation that we will examine, so results for the rate of S will apply to this type of ${}^{C}X$ apart from the factor 2. We will study S and the Monroe ${}^{C}X$ gate.

The Hamiltonian for the ion that is being illuminated by the laser during a given gate is

$$H=H_0+H_I, \tag{7}$$

where H_0 is diagonal, with diagonal elements given by $\hbar(0,\omega_z,2\omega_z,\ldots,\omega_0,\omega_0+\omega_z,\omega_0+2\omega_z,\ldots)$, and the interaction Hamiltonian

$$H_I=\hbar\frac{\Omega}{2}\begin{pmatrix}\mathbf{0} & \hat{C}e^{i\omega_L t}\\ \hat{C}^{\dagger}e^{-i\omega_L t} & \mathbf{0}\end{pmatrix}, \tag{8}$$

where $\hat{C}$ is the matrix having elements C_{nm}. Note that the only approximation so far is to ignore the other vibrational modes.

We first adopt a frame rotating with the laser frequency: $|\tilde{\psi}(t)\rangle=U|\psi(t)\rangle$, where U is a diagonal unitary matrix, with diagonal elements $\exp(i\{-1,-1,-1,\ldots,1,1,1,\ldots\}\omega_L t/2)$. The states $|\tilde{\psi}(t)\rangle$ satisfy the Schrödinger equation $i\hbar(d/dt)|\tilde{\psi}\rangle=\tilde{H}|\tilde{\psi}\rangle$, where $\tilde{H}\equiv i\hbar(dU/dt)U^{\dagger}+UHU^{\dagger}$ is now a time-independent Hamiltonian. We can therefore write the solution to the Schrödinger equation

$$|\tilde{\psi}(t)\rangle=e^{-i\tilde{H}t/\hbar}|\tilde{\psi}(0)\rangle\equiv V^{\dagger}e^{-iV\tilde{H}V^{\dagger}t/\hbar}V|\tilde{\psi}(0)\rangle, \tag{9}$$

where V is the matrix of eigenvectors of $\tilde{H}$, so that $V\tilde{H}V^{\dagger}$ is diagonal.

The quantity of interest, from the point of view of quantum information processing in the trap, is the final state expressed as a superposition of computational basis states. If at

$t=0$, the computational basis states are $|\tilde{u}(0)\rangle=|u(0)\rangle$, then at other times they are $\exp(-i\tilde{H}_0 t/\hbar)|\tilde{u}(0)\rangle$ since then the coefficients $\langle\tilde{u}(t)|\tilde{\psi}(t)\rangle$ do not evolve in the absence of gate operations. Therefore, we would like to calculate

$$\langle u(0)|e^{-i(\tilde{H}-\tilde{H}_0)t/\hbar}|\psi(0)\rangle. \tag{10}$$

Define $P\equiv\exp[-i(\tilde{H}-\tilde{H}_0)t/\hbar]$, and let G be the precise unitary operator for the intended gate. Then the degree to which the laser pulse produces the intended gate is given by the overlap between the final state and one that would be obtained from G. To indicate the degree of imperfection of the laser pulse operation, we therefore calculate

$$f_{\min}=\min_{\psi}|\langle\psi|G^{\dagger}P|\psi\rangle|^2 \tag{11}$$

and define the imprecision to be $\epsilon=(1-f_{\min})^{1/2}$.

Let us comment on whether or not $\epsilon\neq 0$ represents imperfection in the system. We are assuming no imperfection in the sense of unknown dynamics (e.g., laser intensity and frequency noise). Therefore, as long as we can calculate numerically the effect of the laser pulse operation, we have accurate knowledge of the expected state of the system: the fact that the laser pulse gate differs from any particular ''ideal'' gate is not a source of any imprecision at all. However, the intention is to use the ion trap as a quantum processor, to do quantum calculations that we lack the computing power to simulate classically. Putting together many laser pulses, we are therefore assuming we cannot predict the effect on the whole quantum process of having $\epsilon\neq 0$ in all the operations. Therefore ϵ must be regarded as imprecision in the device, which must be minimized.

The question of driving complicated evolution in a predictable manner is central to other techniques such as NMR spectroscopy, and there exist methods to combine pulses causing different types of driven rotation in order to undo the effect of certain terms in the Hamiltonian. Equivalent methods can almost certainly be found for the ion-trap system, but in any case operations close to ideal ones will remain the best starting point for any such method.

C. Performance without correction for light shift

In this section, we will examine the operation of the processor in the regime $\eta<1$, in the case that the light shifts (a.c. Stark shifts) are not taken into account when choosing the laser pulse frequency, phase, and duration.

First consider the S gate: a π pulse on the first red sideband. We set $\omega_L=\omega_0-\omega_z$ in (II B), and examine the eigenvalues of $\tilde{H}$. The separations between the eigenvalues enable one to deduce the Rabi flopping frequencies and the light shifts in the system. The Rabi flopping frequency on the $|n=0\rangle\leftrightarrow|n=1\rangle$ transition is $\eta\Omega$, as expected, which confirms that the gate time is $T_S=\pi/(\eta\Omega)$ as in Eq. (4).

The frequency of the transition is shifted by

$$\Delta\omega=\frac{1}{2}\left(1+\frac{\eta^2}{2}\right)\left(\frac{\Omega}{\omega_z}\right)^2\omega_z+\frac{1}{8}\left(\frac{\Omega}{\omega_z}\right)^4\omega_z+\cdots. \tag{12}$$

This is primarily the light shift caused by the presence of $\Delta n=0$ transitions, which are off-resonant by ω_z.

As was noted by Wineland *et al.* [14], the primary error in the gate operation is caused by the light shift $\Delta\omega$, which can be significant compared to the Rabi flopping frequency $\eta\Omega$. To understand its effect, we now model the transition of interest, that is $|g,n=1\rangle\leftrightarrow|e,n=0\rangle$, as a two-level system, driven by a π pulse off-resonant by $\Delta\omega$. The only term in the propagator of first order in $\Delta\omega$ is $i(\Delta\omega/\alpha)\sin(\alpha t/2)$, where $\alpha^2=\eta^2\Omega^2+\Delta\omega^2$. Putting $\eta\Omega t=\pi$, we obtain

$$\epsilon\simeq\left|\frac{i\Delta\omega}{\alpha}\right|\simeq\frac{\Omega}{2\eta\omega_z}. \tag{13}$$

Therefore, to attain a given gate precision ϵ, the Rabi frequency must satisfy $\Omega\leqslant 2\epsilon\eta\omega_z$, which gives

$$\frac{1}{T_S}=\frac{\eta\Omega}{\pi}\leqslant\frac{2\epsilon}{\pi}\eta^2\omega_z \tag{14}$$

$$=4\epsilon\frac{E_R}{Nh}. \tag{15}$$

The result thus has the simple form that the processor speed for swap operations is limited by the N-ion recoil frequency.

Next, consider the ${}^{C}X$ gate using the special Lamb-Dicke parameter method of Monroe *et al.*, that is, a $2m\pi$-pulse on the carrier with $2m=1/\eta^2$. Substituting $\omega_L=\omega_0$ into (II B), and examining the eigenvalues of $\tilde{H}$, we find the transition frequencies are shifted by

$$\Delta\omega\simeq\frac{(\eta\Omega)^2}{\omega_z}. \tag{16}$$

Since $\Delta\omega\ll\Omega$, the light shifts for this gate are much less significant. Modeling each driven transition as a two-level system, using the same method described above for the S gate, we find that the effect of $\Delta\omega$ is $\epsilon\simeq\eta^2\Omega/\omega_z$. This is small compared to the effect of off-resonant excitation of $\Delta n=\pm 1$ transitions. These are driven in the regime where the detuning is large compared to their Rabi frequency, leading to a propagator with terms of order $\sqrt{2}\eta\Omega/\omega_z$, so we find

$$\epsilon\simeq\frac{\sqrt{2}\eta\Omega}{\omega_z}. \tag{17}$$

Setting $\Omega\leqslant\epsilon\omega_z/\sqrt{2}\eta$, we find

$$\frac{1}{T_{C2}}\leqslant\sqrt{2}\epsilon\sqrt{\frac{E_R}{Nh}\frac{\omega_z}{2\pi}},\quad \Omega\ll\omega_z. \tag{18}$$

It might appear from this that the gate speed can increase without limit by using a tight trap, but this is a false impression because the expression is only valid in the regime $\Omega\ll\omega_z$, which means it is only valid for a gate rate that is small compared to $\eta^2\omega_z/\pi\simeq E_R/(Nh)$.

D. Gates with correction for light shift: Red sideband

The light shift is readily corrected for by tuning the laser frequency to accurate resonance with the light-shifted transition frequency [14]. We will now describe the correct laser pulse frequency, phase, and duration, and derive an expression for the imprecision caused by the primary remaining unwanted effect, which is off-resonant excitation. We find that the recoil frequency still strongly influences the processor speed.

We have studied this problem by numerically evaluating expressions (10) and (11). Only vibrational levels with $n<4$ were included, thus yielding an 8×8 propagator matrix. When further vibrational levels were included in the calculation, the results were not significantly affected.

We find that the best implementation of a swap gate is obtained when the laser frequency is tuned to the light-shifted frequency of the first red sideband: $\omega_L=\omega_0-\omega_z+\Delta\omega$, where $\Delta\omega$ is given by Eq. (12). The gate time is still as in Eq. (4). With no further adjustments, this produces a propagator close to $U_\phi S$ where S is a perfect swap operator, and U_ϕ is diagonal with diagonal elements $\exp(i\{1,1,1,\ldots,-1,-1,-1,\ldots\}\Delta\omega T_S/2)$. Therefore, to produce the intended gate, the system must be further evolved by an application of $U_\phi^\dagger$. This is equivalent to applying subsequent laser pulses with a correspondingly adjusted phase. Therefore the swap gate is completed by changing the phase of the oscillator used in the experimental apparatus to keep the laser in step with the atom's internal resonance (at frequency ω_0), by an amount $\Delta\phi=\Delta\omega T_S$.

This adjustment permits the swap gate rate to exceed the recoil frequency. The term in the system propagator P that now gives the dominant contribution to the imprecision ϵ is off-resonant excitation of $\Delta n=0$ transitions. We expect the amplitude for this process to be of order $\Omega/\sqrt{\Omega^2+\omega_z^2}$. Our numerical calculations confirm this, giving

$$\epsilon\simeq\frac{\Omega}{\sqrt{2(\Omega^2+\omega_z^2)}}\simeq\frac{\Omega}{\sqrt{2}\omega_z} \tag{19}$$

for the remaining imprecision in the adjusted swap operation. Therefore, the gate rate is now limited by

$$\frac{1}{T_S}\leqslant 2\sqrt{2}\epsilon\sqrt{\frac{E_R}{Nh}\frac{\omega_z}{2\pi}}, \tag{20}$$

which is $2\sqrt{2}\epsilon$ times the geometric mean of the N-ion recoil frequency and the vibrational frequency of the chosen normal mode.

If an auxilliary transition is available, the above argument will hold for the ${}^{C}Z$ gate implemented by a 2π-pulse to the first vibrational sideband of the auxilliary transition, the only difference is that the gate rate at given ϵ is half that for the SWAP gate ($T_{C1}=2T_S$).

E. Carrier

The Monroe method ${}^{C}X$ gate is executed by a laser pulse at the carrier frequency. The speed limit given by Eq. (18) cannot be exceeded, since it is caused by off-resonant excitation that cannot be avoided. However, we are interested in the behavior outside the region of validity of Eq. (18), that is, when $\Omega\sim\omega_z$.

When η is small but Ω is not, the precision of the operation need not be limited by off-resonant excitation of $\Delta n=\pm 1$ transitions, since their rate is low. The source of imprecision instead comes from the fact that the dynamics of the system can no longer be pictured as separate Rabi flopping on the $n=0\leftrightarrow 0$ transition and the $n=1\leftrightarrow 1$ transition. Rather, the interaction Hamiltonian drives the set of vibrational levels $n=0,1,2,\ldots\sim\Omega/\omega_z$ as a single entity. The result is that the evolution from an initial state $|n=0\rangle$ is almost the same as the evolution from an initial state $|n=1\rangle$. Therefore the Rabi flopping must be driven for a longer time before a ${}^{C}X$ gate is obtained, and the gate speed ceases to increase with Ω. The rate obtained at $\Omega\sim\omega_z$ was found to be the maximum. Recalling the expression (6) for T_{C2}, it is seen that this maximum is approximately the recoil frequency.

In the region $\Omega\sim\omega_z$, the gate can be optimized simply by adjusting the pulse duration. The correct pulse length is not precisely $\pi/(\eta^2\Omega)$, but differs from this by an amount of order $\pi/(\eta\Omega)$. We have not found any simple expression for this adjustment, we surmise that this is because it is a complicated function of all the light shifts in the multi-level system. To run a processor in practice, the correction to the gate time can either be calculated numerically, or measured experimentally. By this adjustment, we were able to extend the region of validity of expression (18) up to $\Omega\simeq 0.5\omega_z$. Operating at this limit, the gate rate is always equal to the N-ion recoil frequency, independent of the trap tightness, but the gate becomes more precise as the trap gets tighter [$\epsilon\simeq\eta/\sqrt{2}$, expression (17)].

One way to use the carrier excitation method to achieve faster ${}^{C}X$ gates, is to use higher vibrational levels such as $|n=2\rangle$ (in conjunction with $|n=0\rangle$). However, this would mean that the S gate would have to drive the second red sideband, making it slower (the expected limitation at small η being off-resonant excitation of $\Delta n=0$ transitions). Therefore only small gains, if any, are available by this route.

F. Sensitivity to laser-intensity fluctuations

Although our main purpose is to study limitations imposed by the unavoidable properties of the system, we comment here on the sensitivity to one source of technical noise, namely laser intensity fluctuations, since these partially limit our experiments described in Sec. III. The laser drives Rabi flopping at frequency $\eta\Omega$ for the Cirac-Zoller swap gate, and at frequency Ω for the Monroe gate. If, owing to intensity fluctuations, Ω is imprecise by $\Delta\Omega$ then the action of either gate will be imprecise by $\epsilon\simeq T_S\eta\Delta\Omega/\pi$ and $\epsilon\simeq T_{C2}\Delta\Omega/\pi$, respectively. We therefore find $\Delta\Omega/\Omega\simeq\epsilon$ for the swap gate (also for the closely related ${}^{C}Z$ gate), whereas $\Delta\Omega/\Omega\simeq\eta^2\epsilon$ for the Monroe gate.

G. Allowance for all the normal modes

The only approximation we made was to neglect all but one of the normal modes of oscillation of the ion string.

When we relax this assumption, the main features of the more general problem can be understood in terms of the Rabi frequencies and the normal mode frequencies. To keep the notation clear, we will describe a case of three normal modes, which we will label *x*, *y*, and *z*, but the discussion readily generalizes to more normal modes. In our experiments described in Sec. III, there is a just a single ion, so the modes of interest are indeed vibration along the principal axes of the trap, but the modes here labeled *x*, *y*, and *z* could equally refer to different normal modes of the *z* oscillation of a three-ion string, in the case where the two other directions of oscillation are frozen out owing to the linear geometry (that is, they have much higher frequency, and are prepared in the ground state). Equation (2) is replaced by

$$\Omega(n_x,m_x)(n_y,m_y)(n_z,m_z) = C_{n_x m_x}(\eta_x) C_{n_y m_y}(\eta_y) C_{n_z m_z}(\eta_z)\Omega \qquad (21)$$

in an obvious notation, where we now redefine $\Omega \equiv \exp[-(\eta_x^2+\eta_y^2+\eta_z^2)/2]\Omega_{\text{free}}$. There are two regimes to consider. In the case that all the modes are prepared very close to the ground state, the main effect is that the light shift is no longer that given by Eq. (12), but one given by a sum of light shifts related to all the possible transitions. This is easily compensated by a suitable adjustment to the laser frequency. The limit on precision therefore remains that due to off-resonant transitions. For excitation on the red sideband ($n_z=0$, $m_z=1$), in addition to carrier transitions excited off-resonant by ω_z with Rabi frequency Ω, there are also sideband transitions excited off-resonant by $\omega_x-\omega_z$ and $\omega_y-\omega_z$, with Rabi frequencies $\eta_x\Omega$ and $\eta_y\Omega$, respectively. Since the latter contribute at a higher order in η compared to the carrier term, they are negligible unless two modes are close in frequency. For a linear ion string, the separation of the lowest mode frequencies is large enough that the additional terms make little contribution. Therefore our previous discussion, including Eqs. (19) and (20), remains valid. In the experiments described in Sec. III, on the other hand, $\omega_y-\omega_z \simeq 0.025\omega_z$ so unwanted excitation of the *y* sideband has to be taken into account.

For the carrier excitation, in addition to the *z* sidebands excited off-resonant by ω_z with Rabi frequency $\eta_z\Omega$, there are also sideband transitions excited off-resonant by ω_x and ω_y with Rabi frequencies $(1-\eta_z^2)\eta_x\Omega$ and $(1-\eta_z^2)\eta_y\Omega$, respectively. These contribute at the same order in η as the *z* sidebands, and result in a change to Eq. (18) by a numerical factor of order unity.

Our experiments were carried out with only one mode cooled to the ground state. The other two modes had roughly thermal distributions with mean vibrational quantum number of order 10. The result of this is to blur all the Rabi frequencies and light shifts, since each time a given *z* transition is excited, the Rabi frequency depends on the *x* and *y* vibrational quantum numbers

$$\Omega(n_x,n_x)(n_y,n_y)(n_z,m_z) \simeq (1-n_x\eta_x^2)(1-n_y\eta_y^2)C_{n_z m_z}\Omega. \qquad (22)$$

We are able to fit our experimental results by calculating the evolution for each value of n_x, n_y, and then averaging over a thermal population of the *x* and *y* vibrations.

H. Summary

In conclusion, we find that the swap gate and the Cirac-Zoller type of controlled-phase gate can be made faster, at a given level of precision, by making the trap tighter, but the speed increase is only in proportion to $\omega_z^{1/2}$. This is in agreement with earlier work [4], but here we have added a precise quantitative statement of the tradeoff between speed and precision. Some previous studies have adopted $T_S \sim \pi/\omega_z$ for the purpose of making rough estimates, but we find the error thus introduced is significant; for example, it leads to an overestimate of the switching rate by two orders of magnitude in [15]. By exciting the ion in the node of laser standing wave, it is possible to avoid (or greatly reduce) the off-resonant carrier excitation [1,7], therefore $T_S \sim \pi/\omega_z$ may be available, but this involves a significant extra complication of the experiment that may render it unfeasible in practice [16].

The ''magic Lamb-Dicke parameter'' method of Monroe *et al.* cannot be speeded up indefinitely, it has a natural speed limit given by the recoil frequency.

There are advantages in having the ions spaced by a micron or more, in order to allow laser addressing of one ion at a time, and/or resolving the fluorescence from different ions with appropriate imaging optics [17]. If we set a limit *s* for the smallest permissible seperation of the closest ions in the string during processing, we obtain [15,4]

$$\omega_{z,\text{cm}}^2 < \frac{8e^2}{4\pi\epsilon_0 M s^3 N^{1.71}}. \qquad (23)$$

Putting this in Eq. (20), and adopting the breathing mode $\omega_z = \sqrt{3}\omega_{z,\text{cm}}$, we obtain for the fastest swap gate rate, at given precision and ion spacing,

$$\frac{1}{T_S} \simeq 2.5\left(\frac{e^2}{4\pi\epsilon_0}\right)^{1/4} \epsilon \left(\frac{E_R}{h}\right)^{1/2} \frac{1}{M^{1/4} s^{3/4} N^{0.93}}. \qquad (24)$$

If we approximate the N dependence as N^{-1}, and set $s = 10\lambda$ where λ is the laser wavelength, then we arrive at a ''gate time per ion'' that depends only on the choice of ion and transition, at given ϵ. This quantity, T_S/N, is given in Table II for some example transitions, for the case of 99% gate fidelity (i.e., $\epsilon = 0.1$).

III. EXPERIMENTS

In this section, we describe our experimental investigations, carried out in conditions where the Rabi frequency $\Omega_{\text{sideband}} \equiv \eta\Omega_{\text{carrier}}$ of the sideband excitation is significantly above the recoil frequency. We thus are able to investigate the regime where the speed of execution of the gates determines the fidelity of operation.

We use a single trapped $^{40}Ca^+$ ion to demonstrate the principle of quantum information processing. The electronic

TABLE II. Relevant parameters for the implementation of quantum information in trapped ions: wavelength, recoil frequencies for qubit candidate ions, assuming 45° angle between laser wave vector and the z axis. Minimum gate time per ion for 99% fidelity SWAP gates, for three example transitions. The gate time per ion, T_S/N, is given by Eq. (24), for the case $\epsilon=0.1$, $s=10\lambda\simeq 3,4,7$ μm.

Ion	Mass	Qubit Basis	Transition	Recoil Frequency (kHz)	Gate Time Per Ion (μs)
Beryllium	9	hyperfine ground states F=2 F=1	313 nm Raman	452	1.26
Calcium	40	Zeeman ground states $S_{\pm 1/2}$	397 nm Raman	63	5.6
Calcium	40	$S_{1/2}$ ground and $D_{5/2}$ metastable state	729 nm single-photon	4.7	34

$|S_{1/2},\ m=-1/2\rangle$ ground state and the metastable $|D_{5/2},\ m=-5/2\rangle$ state (1s lifetime) are used to implement one qubit. We apply a 4-Gauss bias magnetic field to lift the degeneracy of sublevels in the ground- and excited-state manifolds. The qubit can be coherently manipulated by laser light at 729 nm (see Table II). Two basic operations are demonstrated. First there is the single-qubit rotation that only affects the individual internal electronic state, and secondly, we perform the swap operation that entangles the electronic state of the ion and its vibrational state. We did not investigate the Monroe *et al.* ^{C}X gate because our experiments involved small Lamb-Dicke parameters of order 0.045. In this regime, the Monroe method is $\sim$500 times more sensitive than the Cirac-Zoller method to laser intensity noise and thermal populations in spectator modes, and we found it to be unworkable in these experiments.

We store the ion in a conventional spherical-quadrupole Paul trap with trap frequencies $\omega_{x,y,z}=2\pi(4.0,1.925,1.850)$ MHz. To acquire each experimental data point, at given values of the parameters, we run a series of 100 cycles. A single experimental cycle is made up of five stages, which are (i) Doppler cooling, (ii) sideband cooling, (iii) coherent driven evolution, (iv) observation of fluorescence, and (v) deshelving. We then record the fraction P_D of the 100 cycles in which fluorescence was observed in the penultimate stage.

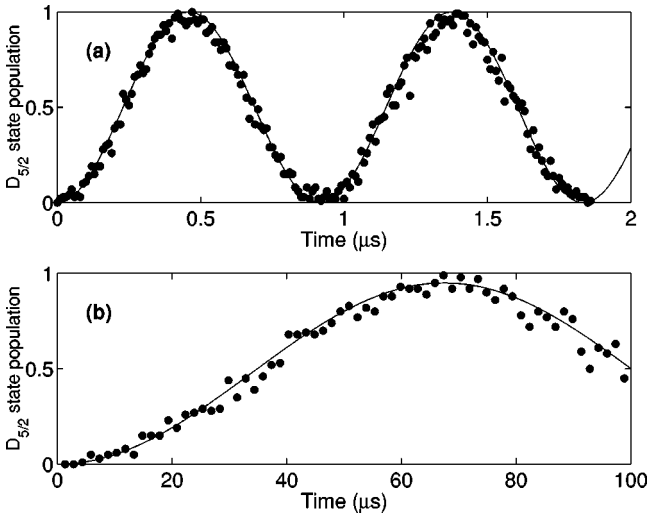

FIG. 1. (a) Rabi oscillations on the carrier. We excite the $\Delta n=0$ transition with a laser power of 100 mW and observe a $\Omega=(2\pi)1090$ kHz Rabi frequency. A contrast of better than 95% is reached for π and 2π pulses. (b) Rabi oscillations on the blue sideband at 4 mW excitation power. At this low power the contrast for π and 2π pulses is 95% and 80%, respectively.

In more detail, the five stages of a cycle are as follows. Doppler cooling is performed on the $|S_{1/2}\rangle$ to $|P_{1/2}\rangle$ 397-nm electric dipole transition. The electronic ground state is then prepared in a pure $|S_{1/2},m=-1/2\rangle$ state by optical pumping. The ion is cooled to the vibrational ground state of the ω_z mode by applying sideband cooling on the $|S_{1/2},m=-1/2\rangle\leftrightarrow|D_{5/2},m=-5/2\rangle$ electric quadrupole transition at 729 nm. A full description of the trap and the cooling procedure is given in Ref. [6]. The wave vector **k** of the 729-nm radiation is nearly perpendicular to the y direction, and has an angle of 40° and 50° to the z and x directions. The corresponding values of $\eta_{x,y,z}^{729nm}$ are (0.04,0.01,0.045). In the qubit operation step, the $|S_{1/2},m=-1/2\rangle\leftrightarrow|D_{5/2},m=-5/2\rangle$ transition is excited with a laser pulse of well-controlled frequency, intensity, and timing. Then, by monitoring fluorescence at 397 nm under laser excitation, we detect whether a transition to the nonfluorescing state $D_{5/2}$ occurred. The scheme allows one to discriminate between the internal states of the ion with an efficiency close to 100% [18–20]. In our experiment, the discrimination effiency is approximately 99.8%, limited by the lifetime of the metastable state [21].

Finally, the ion is again repumped (deshelved) from the $D_{5/2}$ level to the electronic ground state via the $P_{3/2}$ level. The fraction P_D of cycles in which fluorescence is observed

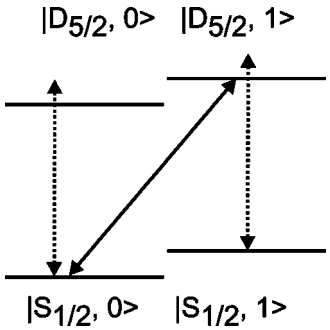

FIG. 2. Relevant energy levels: $|S_{1/2},n=0\rangle$, $|D_{5/2},n=0\rangle$, $|S_{1/2},n=1\rangle$, and $|D_{5/2},n=1\rangle$. The solid arrow indicates the blue sideband excitation, the dotted one the off-resonant carrier excitation.

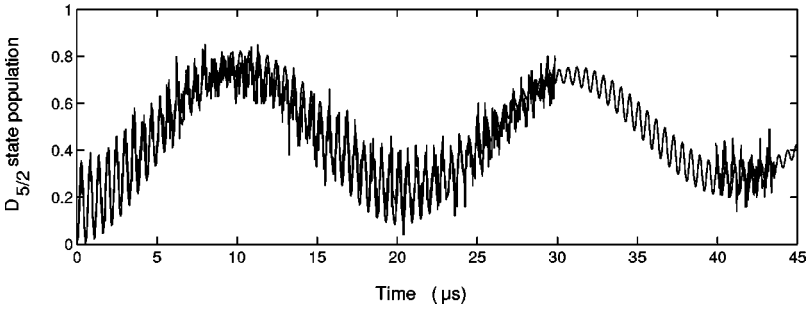

FIG. 3. Rabi oscillation on the blue sideband at 100 mW excitation laser power. See text for details.

indicates the population of the $D_{5/2}$ level after the coherent qubit operation step.

A. Carrier excitation

As discussed in Sec. II A, the single-qubit rotation can be driven fast and without loss in contrast, even in the range where Ω exceeds the trap frequencies $\omega_{x,y,z}$, as long as the Lamb-Dicke parameters are sufficiently small. To reach this limit in the case of a single-photon transition under traveling wave excitation, the wave vector **k** of the exciting light field should be perpendicular to the chosen vibration direction, and to the direction having next smallest vibrational frequency. The remaining vibrational frequency must be large compared to Ω. In our case, the laser is nearly perpendicular to one of the weak confinement directions, but not the other, so there is some unwanted excitation of the motion. A limit to execution speed is set by the available laser power to drive the qubit transition. However, Rabi frequencies as high as a few MHz can be achieved even in the case of dipole forbidden quadrupole transitions.

Rabi oscillations on the $\Delta n=0$ carrier transition at a frequency $\Omega_{\text{carrier}}=2\pi 1090$ kHz are shown in Fig. 1(a). For this, 100 mW of light are focussed into a waist of 30 μm at the position of the ion. We observe a contrast of more than 95%, the contrast being mainly limited by the thermally distributed axial vibration mode ($\omega_x=2\pi 4.0$ MHz), which causes a spread in Rabi frequency owing to the *n* dependence as indicated in Eq. (22). We find that our results are consistent with an average over a thermal phonon distribution in the *x* oscillator having $\langle n\rangle=12(2)$.

B. Sideband excitation

The second building block is the sideband excitation, involving a $\Delta n\neq 0$ transition, here performed on the *z* vibration. For convenience, we adopted the first blue rather than red sideband. The equivalence of blue and red sidebands for these studies was mentioned in Sec. II A. The laser frequency was red-detuned from the blue sideband resonance (measured at low laser power) to compensate for the a.c. Stark effect. The accuracy of the $\Delta n=+1$ operation is therefore limited by off-resonant excitations on the $\Delta n=0$ transition, as discussed in Sec. II D (see also Fig. 2). We indeed observe off-resonant carrier excitation, visible as fast oscillations with a frequency near ω_z on top of the $\Omega_{sideband}=2\pi 48$ kHz Rabi oscillation (see Fig. 3). Note that this frequency is far beyond the recoil frequency, and thus the contrast shrinks to 75% for a π pulse.

If the blue sideband ω_z is excited at a Rabi frequency of $\Omega_{\text{sideband}}=2\pi 7.4$ kHz [Fig. 1(b)], the off-resonant carrier excitation is no longer detectable. A contrast of 95% for a π pulse and 85% for a 2π pulse is measured, while Eq. (19) predicts $\epsilon=0.063$ and hence a fidelity 99.6% for the π pulse. Under low-power excitation, we do not observe any light shift.

The experimental data can be fitted by numerically solving the Schrödinger equation in the truncated basis of the four-level system consisting of $|S_{1/2},n=0\rangle$, $|D_{5/2},n=0\rangle$, $|S_{1/2},n=1\rangle$, and $|D_{5/2},n=1\rangle$ states (see Fig. 2), and averaging over a thermal distribution of population in the other vibrational modes. Three parameters in the calculation were independently measured: the Rabi frequency on the carrier $\Omega=2\pi 1090$ kHz, the Lamb-Dicke parameter η_z, and the trap frequency $\omega_z=2\pi 1850$ kHz. The detuning of the laser field δ is varied for optimum contrast and we find excellent agreement between the data and a numerical simulation for a value of $\delta_{\text{th}}/2\pi=-375$ kHz (Fig. 3). The discrepancy of 125 kHz between δ_{th} and the experimentally determined value $\delta_{\text{exp}}/2\pi=-250$ kHz is probably caused by light shifts due to the $D_{5/2}-P_{3/2}$, $S_{1/2}-P_{1/2}$, and $S_{1/2}-P_{3/2}$ transitions. The

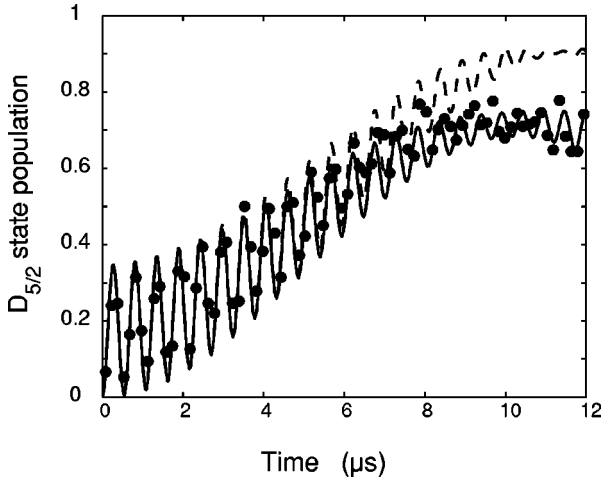

FIG. 4. π pulse on the blue sideband, detailed view. The data of Fig. 3 are plotted together with a fit taking into account a thermally distributed radial *y* mode (see text for the set of parameters). The dotted line gives a prediction for optimized parameters, where all relevant vibration modes are assumed to be cooled to the ground state, and the detuning is set for maximum contrast. A contrast of 92% is predicted under these optimum conditions, and the fidelity $1-\epsilon^2$ given by Eq. (19) would then be 83%.

sum of the calculated light shifts from the dipole transitions is approximately 70 kHz.

A third contribution to the overall light shift is expected from the other radial (y) mode at 1.925 MHz ($\delta\omega/2\pi=75$ kHz). Each level of the y-vibrational ladder is light-shifted, resulting in a change in the $(n_y,n_y)(1_z,0_z)$ z-sideband resonance frequency by approximately $(\eta_y\Omega_{carrier})^2(n_y+1)/[2(\omega_y-\omega_z)]=(n_y+1)(2\pi)0.8$ kHz. Assuming a mean vibrational quantum number of 25, a 20-kHz spread in shifts is expected. To model this situation, we solved the Schrödinger equation for different y-oscillator occupations and averaged the results over a thermal distribution (see Fig. 4). The loss of contrast at $\Omega t=\pi$ is dominated by this thermal averaging, rather than laser intensity and magnetic field fluctuations.

To compare the experimental findings with an optimum π pulse, for a given pulse length, we investigated numerically the parameter space and found that an optimum π pulse (92% contrast of Rabi $|S_{-1/2}\rangle\leftrightarrow|D_{-5/2}\rangle$ oscillation) could be achieved for a detuning of $\delta_{\rm th}/2\pi=-355$ kHz. We conclude that the detuning chosen in the experiment was off by 20 kHz. Note, that the electron shelving detection method only measures the internal-state occupation, *not* the vibrational one. Hence, the measured contrast does not directly yield the fidelity. Equation (19) predicts $\epsilon=0.41$ for this case, and hence a fidelity of 83%. The 20-kHz deviation from the ideal detuning leads to a 5% loss in contrast and the thermally distributed y-vibration mode with $\langle n\rangle=\langle 25\rangle$ further reduces the contrast to 75%. The corresponding fidelity was near 64%. For the details of the π pulse dynamics, see Fig. 4.

To conclude, we have presented a theoretical discussion of two types of quantum gates that couple the internal ion state with its motion, and an experimental study of one of these. Our calculations lead to quantitative statements of the precision of the operations, taking into account the complete Hamiltonian including all the vibrational states and the off-resonant coupling terms. These statements are given in Eqs. (17) and (18) for the Monroe *et al.* ''magic Lamb-Dicke parameter'' gate, and in Eqs. (19) and (20) for the Cirac-Zoller SWAP gate. If we set a limit of a fixed number of laser wavelengths for the spacing of the ions in a linear trap, then we arrive at a gate time per ion, for the SWAP gate, which depends only on the precision and the choice of ion and transition. This time is given in Eq. (24) and Table II.

In our experimental studies, we have demonstrated a contrast of 75% for a $1/T_S=100$ kHz SWAP operation, and 95% for a $1/T_S=14$ kHz SWAP operation on a single trapped ion. These gate rates are, respectively, 21 and 3 times the relevant recoil frequency. In both cases, the contrast could be significantly improved by cooling a further vibrational mode.

[1] J. I. Cirac and P. Zoller, Phys. Rev. Lett. **74**, 4091 (1995).
[2] C. Monroe *et al.*, Phys. Rev. Lett. **75**, 4714 (1995).
[3] Q. A. Turchette *et al.*, Phys. Rev. Lett. **81**, 3631 (1998).
[4] A. M. Steane, Appl. Phys. B: Lasers Opt. **64**, 632 (1997).
[5] C. Monroe *et al.*, Phys. Rev. A **55**, R2489 (1997).
[6] C. Roos *et al.*, Phys. Rev. Lett. **83**, 4713 (1999).
[7] D. V. F. James, Appl. Phys. B: Lasers Opt. **66**, 181 (1998).
[8] D. Deutsch, Proc. R. Soc. London, Ser. A **400**, 97 (1985).
[9] A. Barenco, Contemp. Phys. **37**, 375 (1996).
[10] A. Steane, Rep. Prog. Phys. **61**, 117 (1998).
[11] A. Sorensen and K. Molmer, Phys. Rev. Lett. **82**, 1971 (1999).
[12] K. Molmer and A. Sorensen, Phys. Rev. Lett. **82**, 1835 (1999).
[13] A. Sorensen and K. Molmer, Phys. Rev. A **62**, 022311 (2000).
[14] D. J. Wineland *et al.*, J. Res. Natl. Inst. Stand. Technol. **103**, 259 (1998).
[15] R. J. Hughes *et al.*, Phys. Rev. Lett. **77**, 3240 (1996).
[16] During preparation of this paper, we learned of the work D. Jonathan, M. B. Plenio, and P. L. Knight, e-print quant-ph/0002092, which proposes a method to gain access to the higher speed with traveling wave excitation by making use of the light shift.
[17] H. C. Nägerl *et al.*, Phys. Rev. A **60**, 145 (1999).
[18] T. Sauter, W. Neuhauser, R. Blatt, and P. E. Toschek, Phys. Rev. Lett. **57**, 1696 (1986).
[19] W. Nagourney, J. Sandberg, and H. Dehmelt, Phys. Rev. Lett. **56**, 2797 (1986).
[20] J. C. Bergquist, R. G. Hulet, W. M. Itano, and D. J. Wineland, Phys. Rev. Lett. **57**, 1699 (1986).
[21] C. Roos, Ph.D. thesis, 2000 (unpublished).